

Article

DFT Investigations on the Ring-Opening Polymerization of Trimethylene Carbonate Catalysed by Heterocyclic Nitrogen Bases

Michael Lalanne-Tisné ^{1,2}, Audrey Favrelle-Huret ² , Wim Thielemans ^{1,*}, João P. Prates Ramalho ^{3,*}  and Philippe Zinck ^{2,*} 

¹ Sustainable Materials Lab, Department of Chemical Engineering, KU Leuven, Campus Kulak Kortrijk, Etienne Sabbelaan 53, Box 7659, B-8500 Kortrijk, Belgium

² Université de Lille, CNRS, Centrale Lille, Univ. Artois, UMR 8181—UCCS—Unité de Catalyse et Chimie du Solide, F-59000 Lille, France

³ Chemistry Department, LAQV-REQUIMTE and Hercules Centre, Sciences and Technology School, University of Évora, Rua Romão Ramalho 59, 7000-671 Évora, Portugal

* Correspondence: wim.thielemans@kuleuven.be (W.T.); jpcar@uevora.pt (J.P.P.R.); philippe.zinck@univ-lille.fr (P.Z.)

Abstract: Organocatalysts for polymerization have known a huge interest over the last two decades. Among them, heterocyclic nitrogen bases are widely used to catalyse the ring-opening polymerization (ROP) of heterocycles such as cyclic carbonates. We have investigated the ring-opening polymerization of trimethylene carbonate (TMC) catalysed by DMAP (4-dimethylaminopyridine) and TBD (1,5,7-triazabicyclo[4.4.0]dec-5-ene) as case studies in the presence of methanol as co-initiator by Density Functional Theory (DFT). A dual mechanism based on H-bond activation of the carbonyl moieties of the monomer and a basic activation of the alcohol co-initiator has been shown to occur more preferentially than a direct nucleophilic attack of the carbonate monomer by the heterocyclic nitrogen catalyst. The rate-determining step of the mechanism is the ring opening of the TMC molecule, which is slightly higher than the nucleophilic attack of the TMC carbonyl by the activated alcohol. The calculations also indicate TBD as a more efficient catalyst than DMAP. The higher energy barrier found for DMAP vs. TBD, 23.7 vs. 11.3 kcal·mol^{−1}, is corroborated experimentally showing a higher reactivity for the latter.

Keywords: organocatalysis; ring-opening polymerization; cyclic carbonate; mechanism



Citation: Lalanne-Tisné, M.; Favrelle-Huret, A.; Thielemans, W.; Prates Ramalho, J.P.; Zinck, P. DFT Investigations on the Ring-Opening Polymerization of Trimethylene Carbonate Catalysed by Heterocyclic Nitrogen Bases. *Catalysts* **2022**, *12*, 1280. <https://doi.org/10.3390/catal12101280>

Academic Editor: Ruairaidh McIntosh

Received: 15 September 2022

Accepted: 13 October 2022

Published: 20 October 2022

Publisher's Note: MDPI stays neutral with regard to jurisdictional claims in published maps and institutional affiliations.

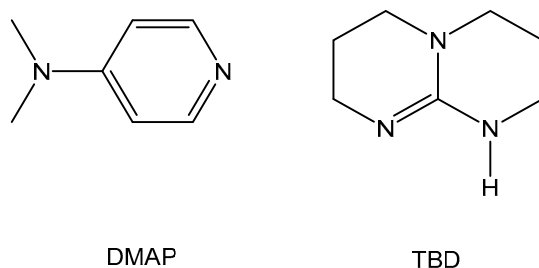


Copyright: © 2022 by the authors. Licensee MDPI, Basel, Switzerland. This article is an open access article distributed under the terms and conditions of the Creative Commons Attribution (CC BY) license (<https://creativecommons.org/licenses/by/4.0/>).

1. Introduction Section

Aliphatic polycarbonates are biodegradable and biocompatible polymers that are used in the biomedical field and as long-chain diols for the synthesis of polyurethanes [1–3]. They can be synthesized by transcarbonatation between a diol and a dialkyl- or diphenyl-carbonate precursor, by epoxide CO₂ alternating copolymerization, or by the ring-opening polymerization of a cyclic carbonate. Both metal-based complexes and organic molecules have been reported as catalysts for these reactions. Among organocatalysts, heterocyclic nitrogen bases have been successfully used for the ring-opening polymerization of cyclic carbonates such as trimethylene carbonate (TMC) [4–6]. TMC is commercially available and can be readily polymerized in comparison to e.g., 5-membered cycles. The reaction can be carried out in solvent as well as in bulk. Using 1,5,7-triazabicyclo[4.4.0]dec-5-ene (TBD, see Scheme 1) as a catalyst in combination with a protic co-initiator, the polymerization is well controlled and occurs without side reactions [4]. Catalyst economy can also be reached via the so-called immortal polymerization, where several equivalents of a protic co-initiator vs. catalyst can be used to efficiently initiate the growth of macromolecular chains. Both TBD and 4-dimethylaminopyridine (DMAP, see Scheme 1) were reported to be effective catalysts for the immortal ROP of TMC [5]. TBD can also initiate the ring-opening polymerization of TMC without a protic co-initiator, leading to a faster polymerization rate

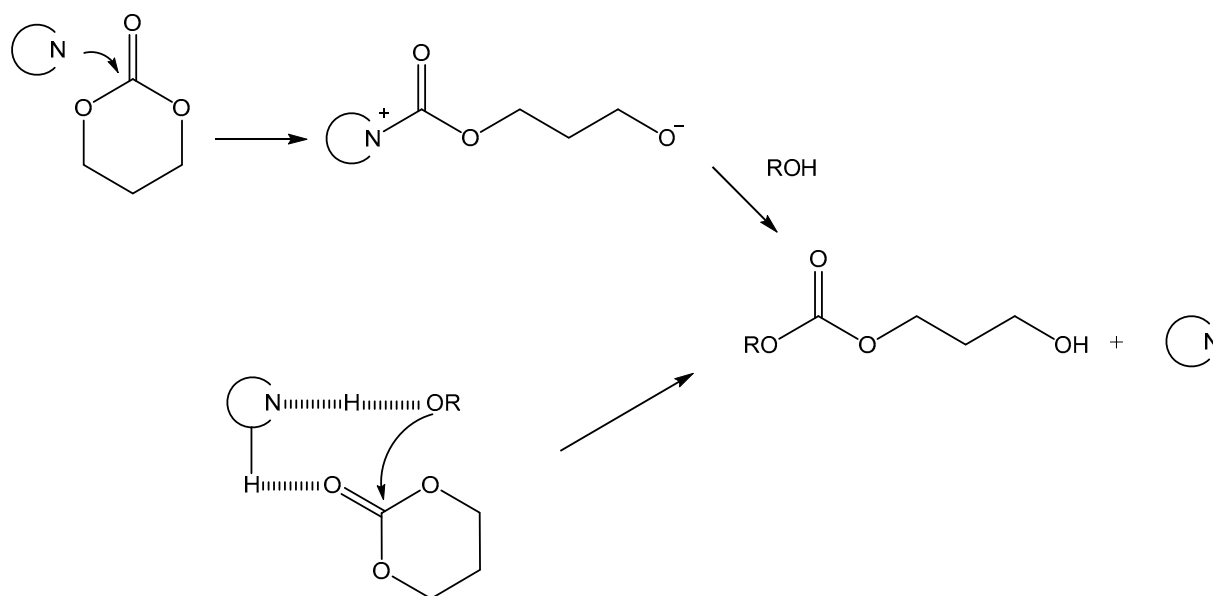
than that observed in the presence of an alcohol, and yielding a mixture of linear and cyclic poly(trimethylene carbonate) macromolecules [6]. The surface functionalization of cellulose nanocrystals by ring-opening polymerization of TMC catalysed by TBD and initiated by the surface hydroxyl groups on the nanocellulose surface is also possible, highlighting the robustness of this catalyst [7].



Scheme 1. Heterocyclic nitrogen bases catalysts considered in this study. From left to right, 4-dimethylaminopyridine (DMAP) and 1,5,7-triazabicyclo[4.4.0]dec-5-ene (TBD).

The mechanisms involved in the ring-opening polymerization of cyclic esters catalysed by *N*-heterocyclic bases have been largely studied by DFT in the literature [8–16] and nicely reviewed recently [17]. Two main mechanisms have been shown to occur: a nucleophilic attack of the catalyst on the carbonyl moieties of the monomer, and a basic activation of a protic co-initiator followed by a nucleophilic attack. The latter mechanism is generally preferred to the monomer nucleophilic activation by the catalyst, as soon as a protic co-initiator is present in the reactive medium. In the case of bases such as TBD, additional H-bond activation of the carbonyl moieties of the cyclic ester has been advanced to occur.

Regarding the ring-opening polymerization of cyclic carbonates, coordination insertion mechanisms have been well discussed based on DFT studies for various metal-based catalysts [18–23]. Theoretical mechanistic insights of organocatalyzed ring-opening polymerizations were in turn devoted to rationalising the polymerization of an *N*-substituted eight-membered carbonate ring [24], to support regioselectivity results of the polymerization of carbohydrate-based carbonates [25–27] or to explain the absence of reactivity observed using a Brønsted pair as catalyst [28]. Elucidation of the basic steps of the mechanism of the ring-opening polymerization of cyclic carbonates catalyzed by organic molecules has surprisingly not been treated in the literature as far as we know. The understanding of these transcarbonatation mechanisms is of prime importance for the optimization of those catalysts, for the development of new catalytic systems, or as a basis for developing efficient copolymerization and chemical recycling strategies. In particular, despite obvious similarities with cyclic esters, the discrimination between the alcohol activation pathway and the direct nucleophilic mechanism of the organocatalyzed ring-opening polymerization of cyclic carbonates catalysed by performant heterocyclic nitrogen bases, as represented in Scheme 2, has never been discussed in the literature. We report in this contribution a DFT investigation of those two mechanisms for the ring-opening polymerization of TMC catalysed by TBD and DMAP as case studies, and corroborate the findings by experimental results.



Scheme 2. Schematic representation of the nucleophilic (upper part) and the alcohol activation/H-bond mechanism (bottom part) for the ring-opening polymerization of TMC catalysed by a heterocyclic nitrogen base and co-initiated by an alcohol.

2. Results and Discussion

2.1. TBD Catalysed Ring-Opening Polymerization of TMC

We started our investigation with the H-bond/alcohol activation pathway for the TBD-catalysed ring-opening polymerization of TMC, co-initiated by methanol. The reaction progresses through two transition states (see Figure 1 and Scheme 3). It is initiated with the formation of a complex with two hydrogen bonds, one between the tertiary amine catalyst nitrogen and the alcohol hydroxyl and the second between the TMC carbonyl oxygen and the catalyst protonated nitrogen. This dual activation of both the alcohol initiator and the carbonate monomer leads to the addition of the MeO moieties to the carbonyl carbon and a hydrogen transfer from the alcohol to the TBD. The structure is presented in Figure 1. This bifunctional activation mechanism leads to an intermediate with a tetrahedral carbon due to the formation of a new oxygen-carbon bond. Remarkably, the **INT1** intermediate consists of two charged moieties ($-0.52e$ the carbonate moiety and $+0.52e$ the protonated TBD moiety) stabilized both by hydrogen bonding and Coulombic interactions. In the second step, a new intermediate adduct **INT2** is formed where a hydrogen bond activates one of the TMC endocyclic oxygens, giving rise to a slightly elongated bond (1.463 \AA , compared with 1.421 \AA for the other endocyclic C-O bond) that, through **TS2** and concomitant transfer of the TBD hydrogen to the endocyclic oxygen, opens the TMC ring and regenerates the TBD catalyst.

Considering the free energy profile depicted in Scheme 3, a barrier height of 11.3 kcal/mol for the ring opening of the TMC molecule is the rate-limiting step of this mechanism, slightly higher than the initial activated nucleophilic attack, with a barrier height of 11.1 kcal/mol , suggesting high plausibility for this mechanism.

The free energy profile for the nucleophilic mechanism is presented in Scheme 4. A nucleophilic attack of the heterocyclic nitrogen TBD catalyst on the carbonyl group of TMC occurs during the first reaction step, with concomitant activation of one of the TMC endocyclic oxygens through hydrogen bonding. This leads to the zwitterionic tetrahedral intermediate **INT1** (Figure 2). The so-formed nitrogen-carbon bond (1.604 \AA) is elongated as well as the endocyclic C-O bond (1.449 \AA) corresponding to the oxygen that shares a hydrogen bond with the TBD catalyst. This intermediate presents a partial charge of $-0.81e$ on the carbonyl oxygen, $-0.66e$ on the endocyclic oxygen ester involved in the hydrogen bond, and $-0.55e$ on the other endocyclic oxygen ester. The ring-opening step proceeds

through **TS2**, with the transfer of the H-bonded hydrogen from the TBD to the oxygen resulting in the formation of a hydroxyl end-capped carbamate.

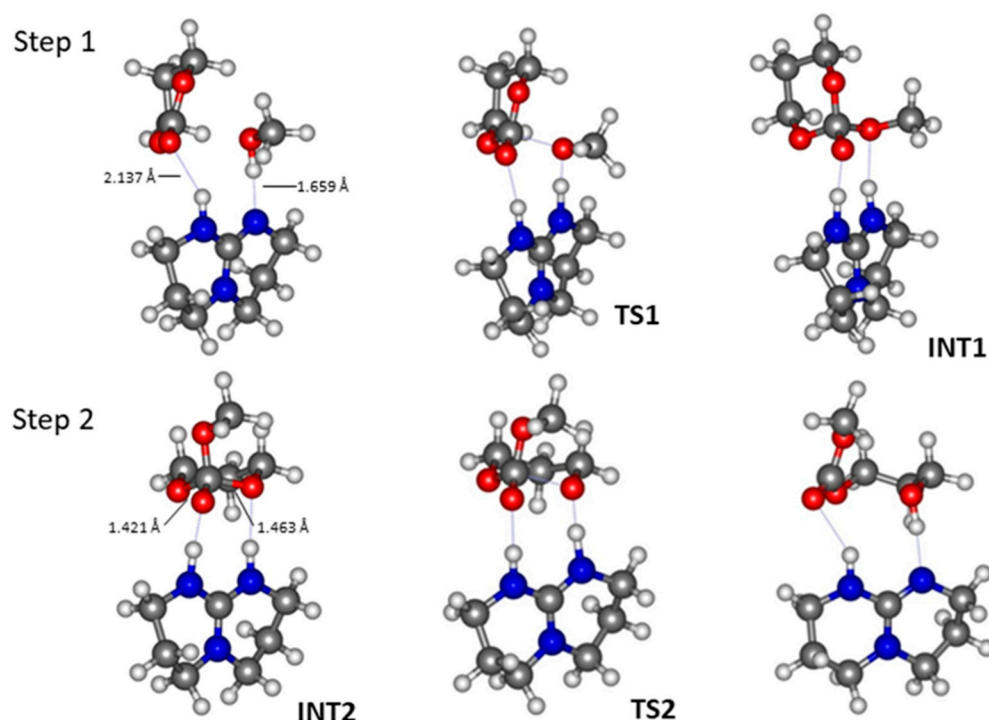


Figure 1. Optimized geometry structures of the species involved in the TBD catalysed ring-opening polymerization for the TMC—H-bond/alcohol activation mechanism. Colour code: C grey, O red, N blue and H white.

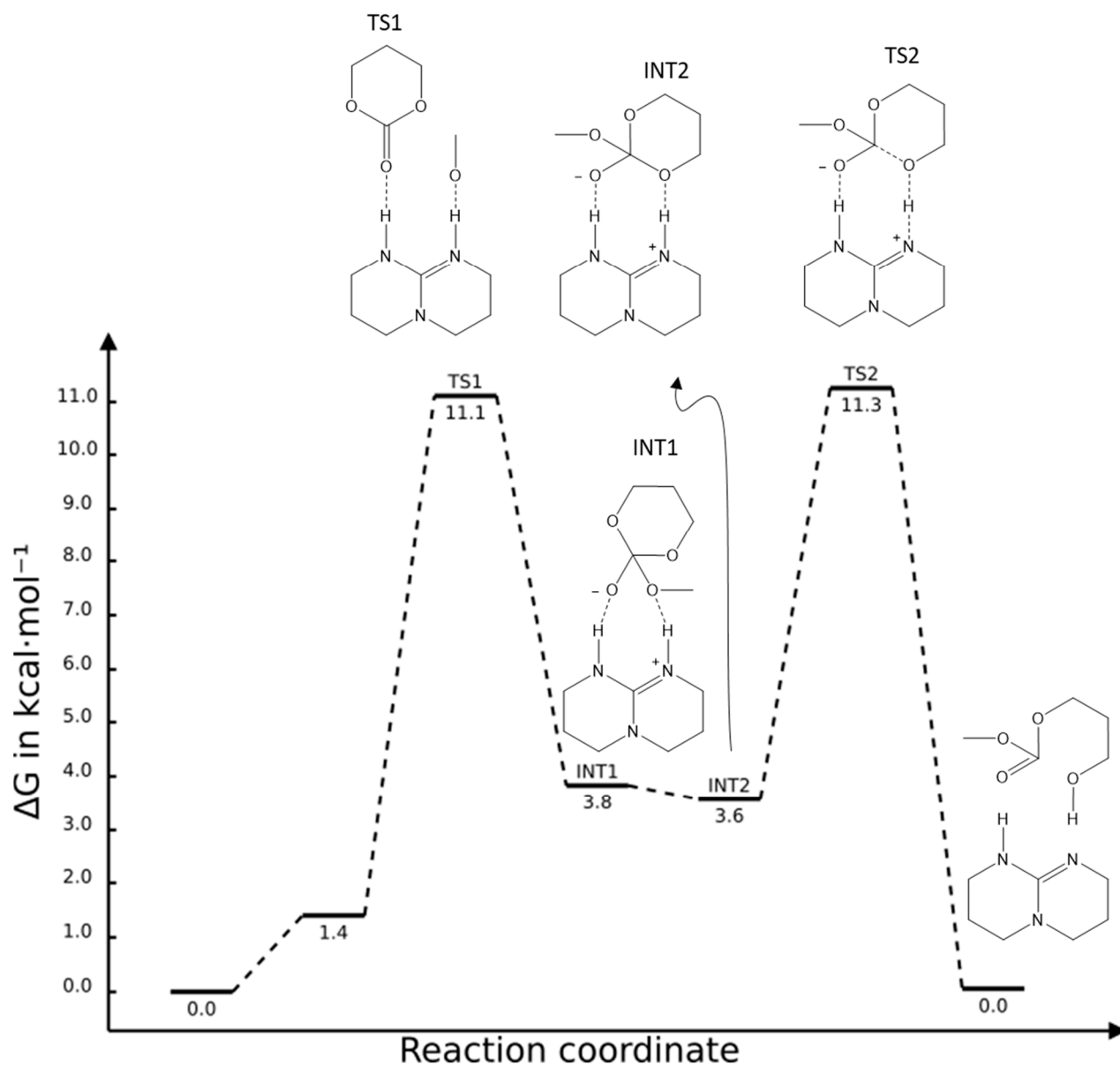
The reaction follows with a catalysed attack of the alcohol on the carbonyl group (**TS3**) and hydrogen transfer of the alcohol hydrogen to the TBD catalyst, which is the rate-limiting step in this mechanism. The associated barrier height of $25.7 \text{ kcal}\cdot\text{mol}^{-1}$ for this mechanism is significantly higher than the $11.3 \text{ kcal}\cdot\text{mol}^{-1}$ obtained for the H-bond/alcohol activation pathway, suggesting that the latter preferentially occurs in the presence of TBD. At this point the elongated nitrogen-carbon bond (1.587 Å) that connects the TBD catalyst with the carbonate moiety promptly dissociates with a small energy barrier corresponding to **TS4**, leading to the separated products and release of the catalyst.

2.2. DMAP Catalysed Ring-Opening Polymerization of TMC

The first step of the H-bond/alcohol activation mechanism in the presence of DMAP is shown in Figure 3, while the free energy profile is given in Scheme 5. The reaction starts with an intermediate **INT1** exhibiting a weak non-classical hydrogen bond of the TMC carbonyl oxygen with one hydrogen atom of the DMAP pyridinium ring ($\text{O} \cdots \text{H}$ 2.367 Å), together with a hydrogen bond of the alcohol with the basic nitrogen of DMAP (N-H 1.747 Å). The so-activated alcohol oxygen is added to the carbonyl carbon while the hydrogen is transferred to DMAP.

With the hydrogen transferred to the DMAP nitrogen and the methoxy oxygen bonded to the TMC carbonyl carbon, an ion-pair character intermediate (**INT2** see Figure 4) with the negative charge mainly located on the TMC oxygens ($-0.88e$ for the carbonyl oxygen, $-0.57e$ and $-0.61e$ for the ester endocyclic oxygens and $-0.48e$ for the methoxy exocyclic oxygen) and a positively ($0.74e$) charged DMAP ring is formed. In addition, the DMAP hydrogenated nitrogen interacts with one of the endocyclic TMC oxygens ($\text{O} \cdots \text{H}$ 1.724 Å) and the TMC carbonyl oxygen with a close ortho-hydrogen atom of the DMAP pyridinium ring, forming a weak nonstandard hydrogen bond ($\text{O} \cdots \text{H}$ 2.213 Å). This results in a slight elongation of the oxygen bond with the carbonyl carbon (1.470 Å , compared with

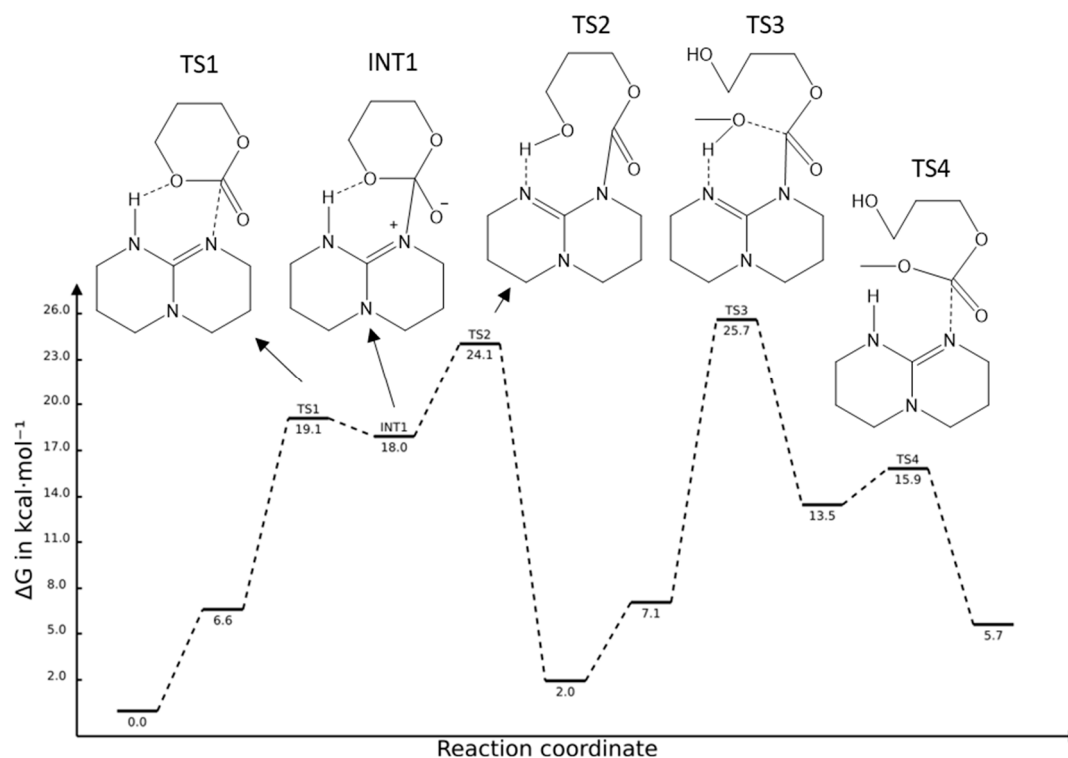
1.432 Å for the other carbonyl carbon endocyclic oxygen bond) that leads to **TS2**. The barrier of 23.7 kcal/mol found for this step makes it the rate-determining step for this mechanism. Finally, a subsequent transfer of the DMAP hydrogen back to TMC leads to the ring opening of the TMC.



Scheme 3. Free energy profile for the TBD catalysed ring-opening polymerization of TMC-H-bond/alcohol activation mechanism.

The free energy profile for the nucleophilic mechanism is presented in Scheme 6. The reaction starts with the formation of a zwitterionic tetrahedral intermediate (**INT1**, see Figure 5), which is only slightly more stable than that of the previous transition state **TS1**. This intermediate possesses an elongated N-C bond (1.659 Å) linking the DMAP pyridinium ring and the carbonyl carbon and presents a partial charge of 0.48e on the DMAP ring, −0.61e on the endocyclic oxygen ester closest to the hydrogen ring, −0.58e on the other endocyclic oxygen ester, and −0.79e on the carbonyl oxygen. The ring opening follows through **TS2** via the linear zwitterionic intermediate **INT2**. In the open ring intermediate the charges modify to 0.61e on the DMAP pyridinium ring, −1.17e on the endocyclic oxygen, −0.56e on the carbonyl oxygen, and −0.43e on the terminal oxygen.

It is interesting to note that the zwitterionic tetrahedral intermediate **INT1** is more stable than the ring-opened zwitterion **INT2**, as tetrahedral zwitterionic intermediates are not usually considered stable species in zwitterionic polymerization reactions [12]. A similar situation has been reported by Waymouth's calculations on the zwitterionic ring-opening polymerization of δ -valerolactone [13].



Scheme 4. Free energy profile for the nucleophilic mechanism of the TBD catalysed ring-opening polymerization of TMC.

This ring-opened zwitterionic intermediate is a highly reactive species and one can speculate that it might react with other TMC molecules leading to the formation of polymers of ring-opened TMC molecules as was suggested by Waymouth for polymerisation of δ -valerolactone [13]. Other possible intermediates are neutral bicyclo species like **BICY1**. Actually, this bicyclo species is 10.8 kcal·mol^{−1} more stable, when compared with the open zwitterion (**INT2**) and 16.1 kcal·mol^{−1} less stable than the **INT1** intermediate. The reaction then proceeds with methanol addition to the carbonyl and concomitant hydrogen transfer to the carbonyl oxygen. This transition state (**TS3**) has a high barrier becoming the rate-limiting step of this mechanism, with a value of 90.3 kcal·mol^{−1}. The H-bond/alcohol activation mechanism, with an energy barrier of 23.7 kcal·mol^{−1}, is thus likely prone to occur in the presence of DMAP.

The ring-opened zwitterion is finally stabilized by a hydrogen transfer through a small energy barrier (Scheme 6), with the formation of the **INT3** intermediate (see Figure 6) where the negative charge is mainly located on the carbonyl oxygens (−0.75e for the carbonyl oxygen and −0.55e and −0.52e for the ester oxygens) closer to the positively (0.48e) charged DMAP ring. Finally, the **INT3** complex, which possesses an extended N–C bond of 1.594 Å promptly dissociates into products through the transition state **TS5** with a tiny barrier of 0.50 kcal·mol^{−1} relative to **INT3**, leading to the reaction products. The free energy difference that one can find in the final products of the two mechanisms (Schemes 5 and 6 as well as in Schemes 3 and 4) reflects the different conformation of the reaction product and the catalyst adducts.

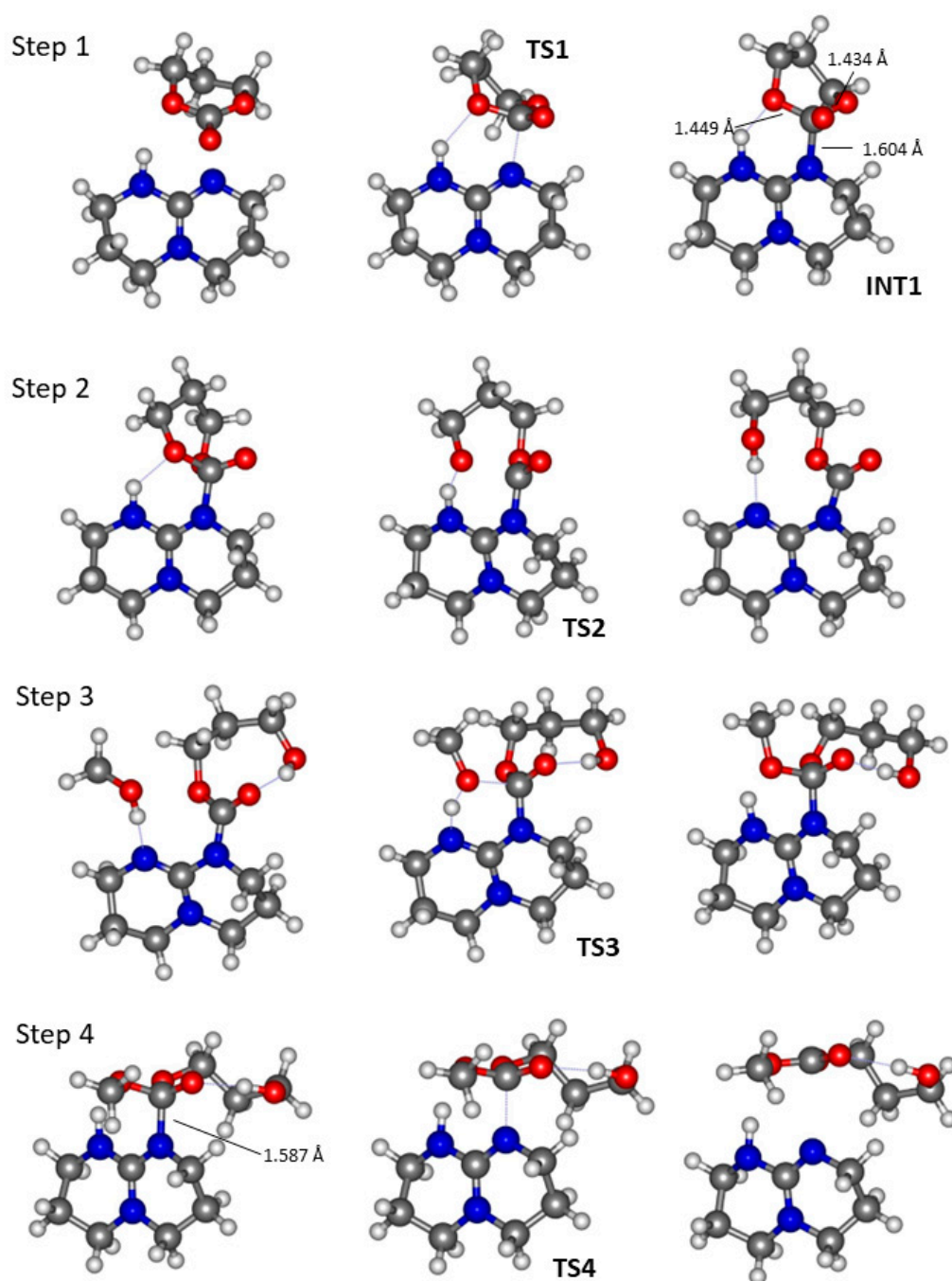


Figure 2. Optimized geometry structures of the species involved in the nucleophilic mechanism for the TBD-catalysed ring-opening polymerization of TMC. Colour code: C grey, O red, N blue and H white.

2.3. Experimental Confirmation

Regarding the more favourable H-bond/alcohol activation mechanism, the highest energy barrier for TBD is 11.3 kcal/mol, which is significantly lower than the energy barrier of 23.7 kcal/mol found for DMAP. This correlates well with the activity of the polymerizations of TMC mediated with these organocatalysts reported in Table 1. In 1 h at room temperature in dichloromethane, the reaction is quantitative using TBD, while only 19% conversion is reached using DMAP.

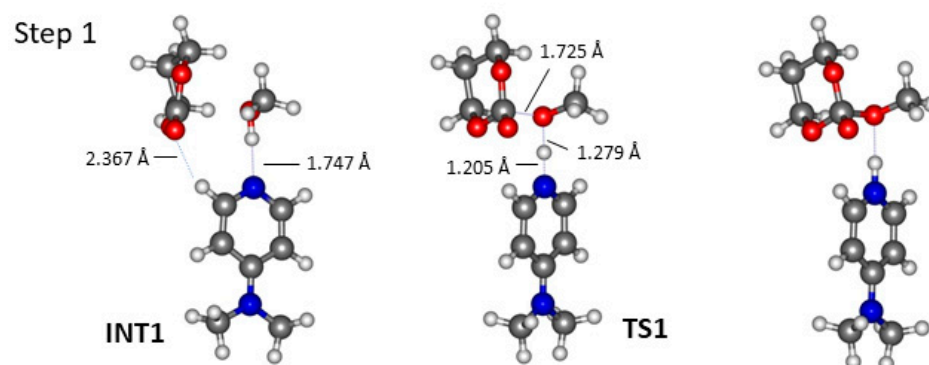
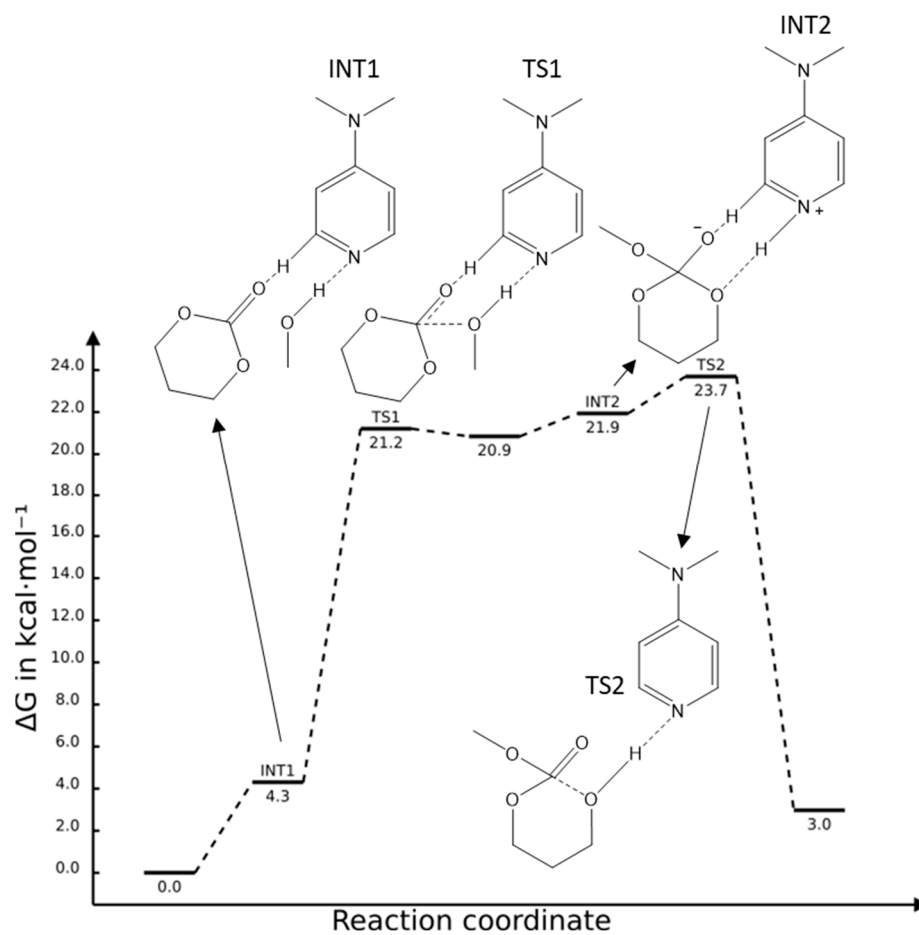


Figure 3. Optimized geometry structures of the species involved in the first step of the H-bond mechanism for the DMAP-catalysed ring-opening polymerization of TMC. Colour code: C grey, O red, N blue and H white.



Scheme 5. Free energy profile for the H-bond/alcohol activation pathway of the DMAP catalysed ring-opening polymerization of TMC.

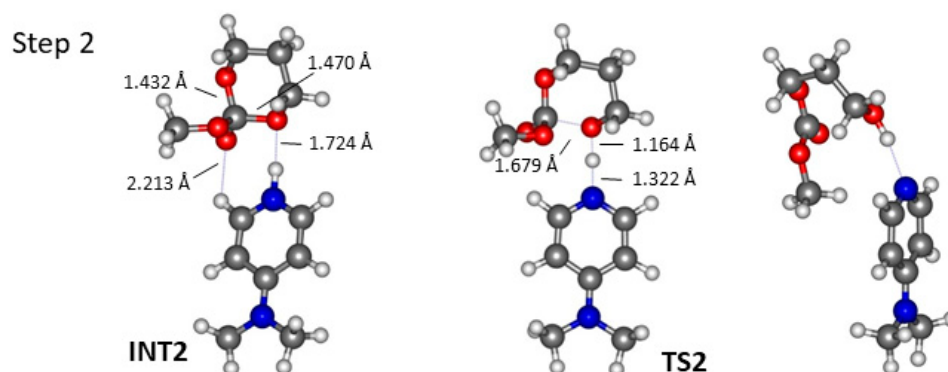
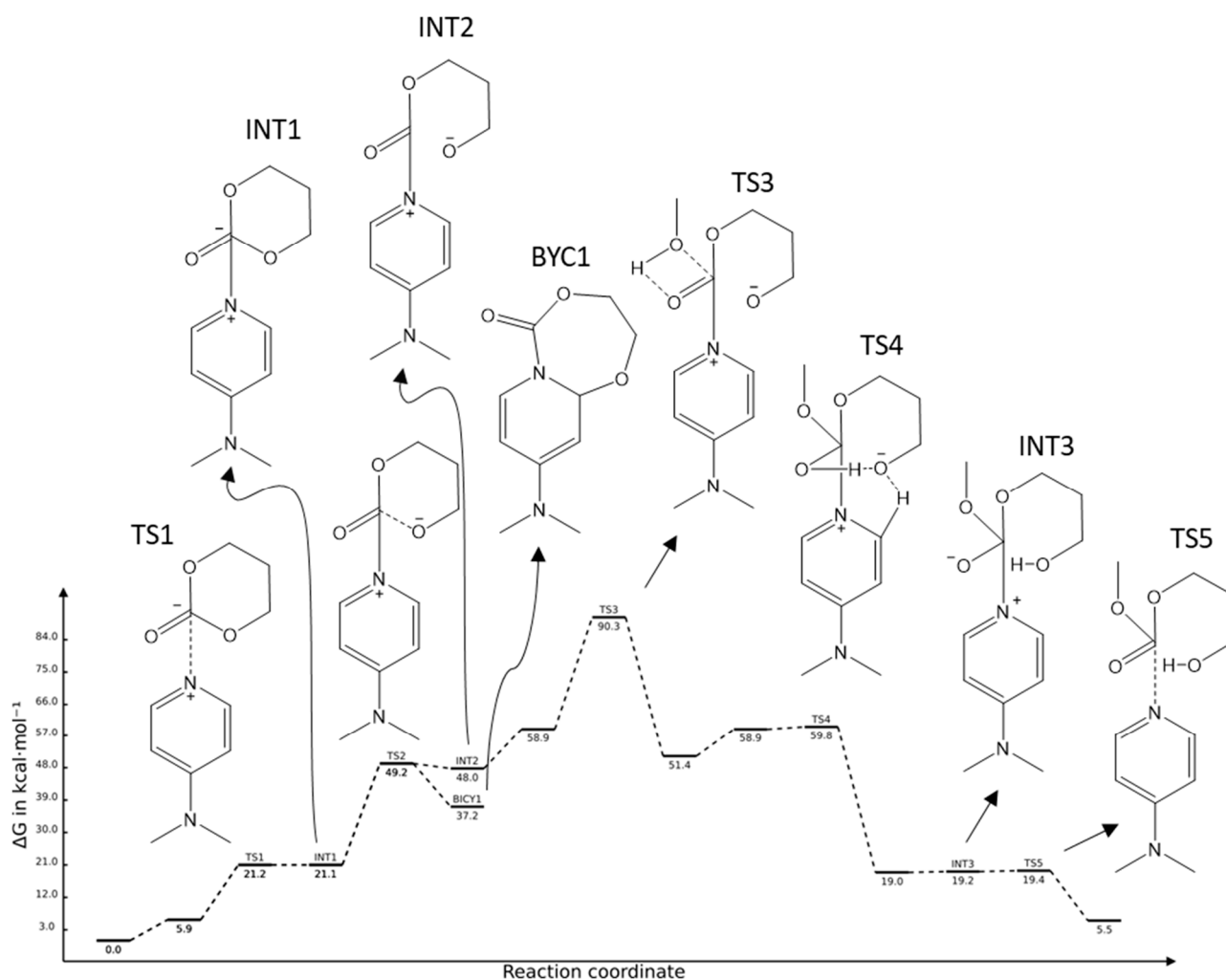


Figure 4. Optimized geometry structures of the species involved in the second step of the H-bond/alcohol activation mechanism of the DMAP-catalysed ring-opening polymerization of TMC. Colour code: C grey, O red, N blue and H white.



Scheme 6. Free energy profile for the nucleophilic path of the DMAP catalysed ring-opening polymerization of TMC.

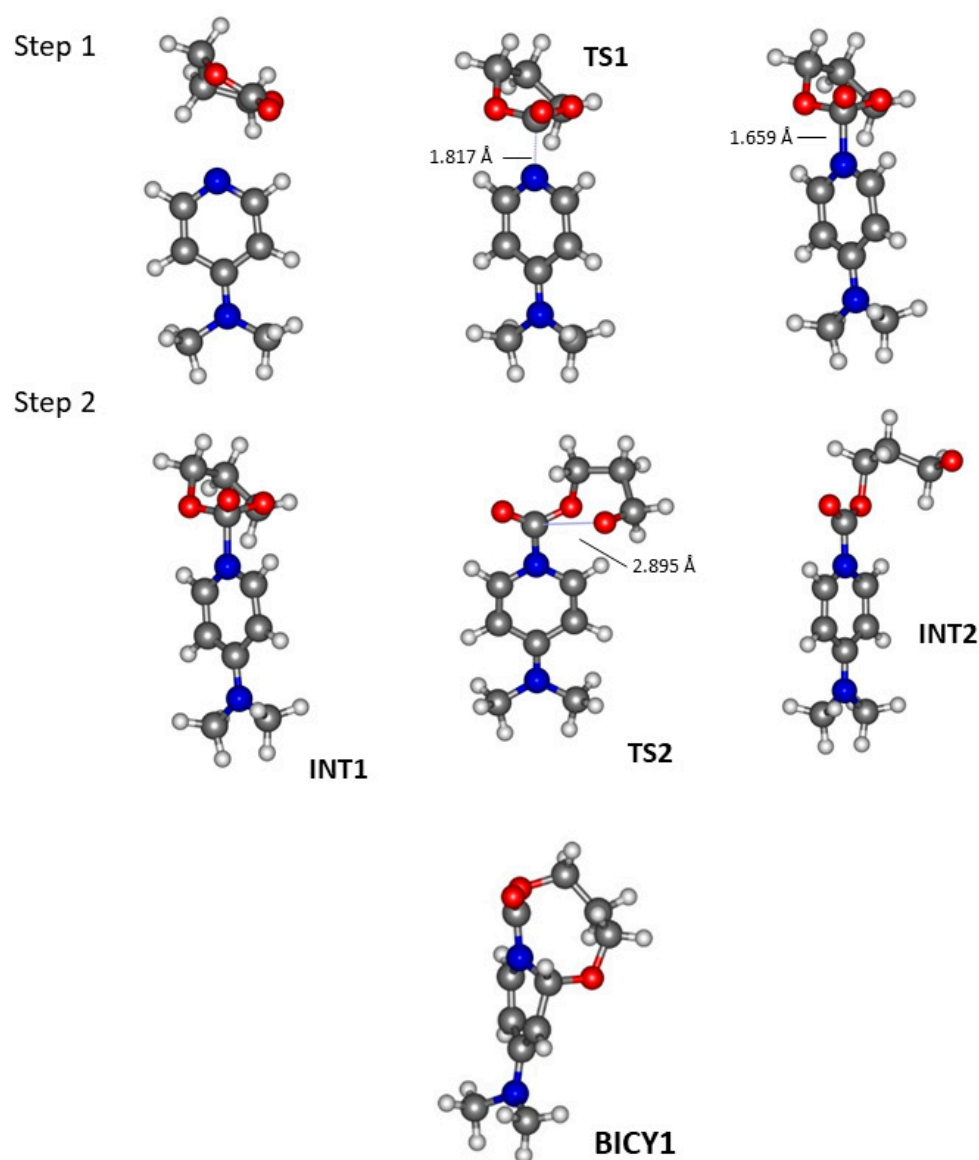


Figure 5. Optimized geometry structures of the species involved in the first and second steps for the nucleophilic mechanism of the DMAP-catalysed ring-opening polymerization of TMC. The structure of a possible bicyclo intermediate species (BICY1) is also displayed (bottom). Colour code: C grey, O red, N blue and H white.

Table 1. Experimental results. Reactions conducted for 1 h at room temperature in 2 mL CH₂Cl₂. TMC/Catalyst/Benzyl alcohol = 100/1/1. ^a determined by ¹H NMR. ^b Number average molecular weight determined by size exclusion chromatography. ^c Dispersity determined by size exclusion chromatography. ^d after reference [4].

Catalyst	Conv. ^a (%)	M _n ^b (g/mol)	Đ _M ^c
DMAP	19	5 500	1.7
TBD ^d	>99	9 900	1.3

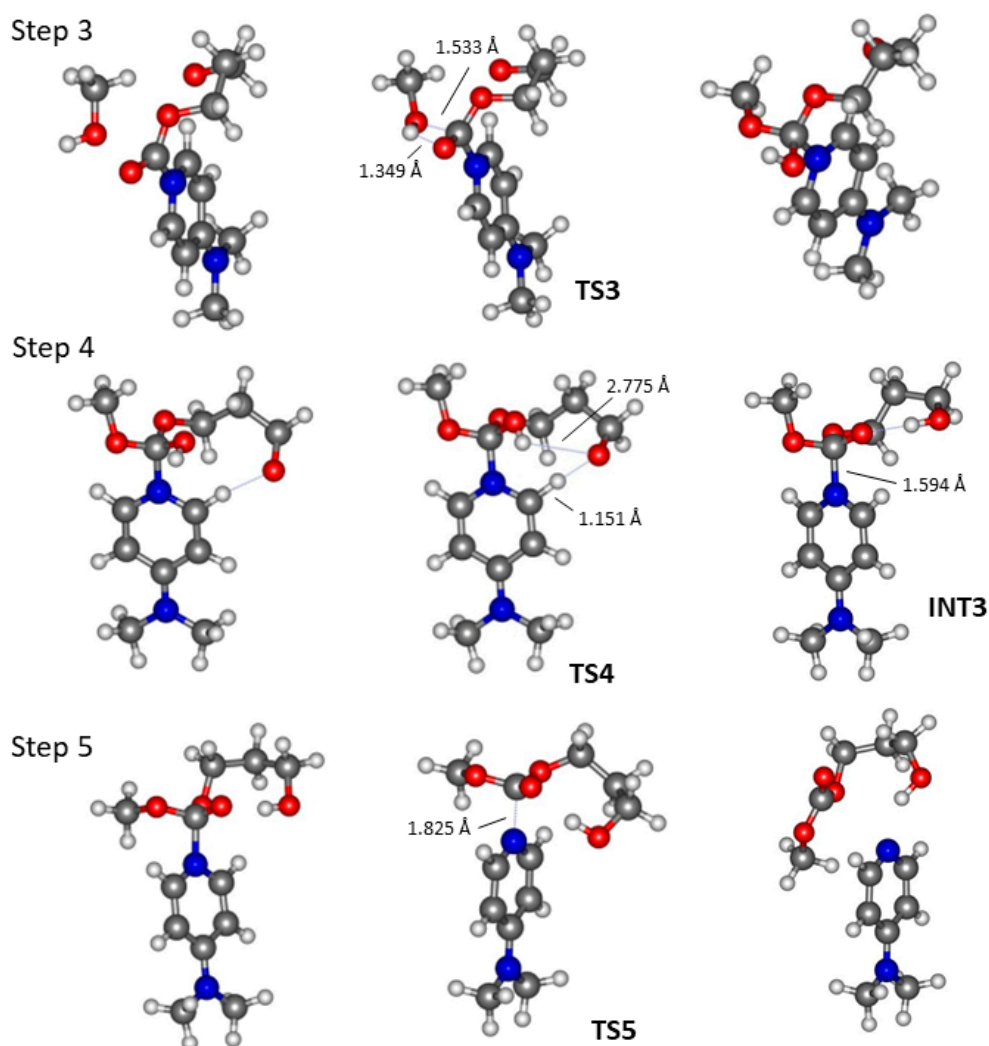


Figure 6. Optimized geometry structures of the species involved in the final steps of the nucleophilic mechanism of the DMAP-catalysed ring-opening polymerization of TMC. Colour code: C grey, O red, N blue and H white.

3. Materials and Methods

3.1. Methodological Details

We adopt a simple model with methanol as a co-initiator, TMC as a cyclic carbonate, and TBD and DMAP as organocatalysts. All calculations in this study were conducted with the Gaussian 16 program package [29]. Geometries of the chemical relevant species were obtained by DFT from optimizations using the hybrid meta-GGA exchange-correlation functional M06-2X [30] together with the 6-31+G(d,p) basis set. The choice of this functional was determined by its broad applicability and remarkable performance in many areas of chemistry including thermochemistry and reaction kinetics, providing reliable energies and barrier heights while considering midrange noncovalent interactions [30–32]. In all calculations, the solvent effects were considered by using the SMD continuum solvation model [33] with the parameters of dichloromethane. Frequency analysis confirmed optimized geometries as energy minimum by the non-existence of imaginary frequencies or as transition states by the existence of a sole imaginary frequency that links reactants and products along the reaction coordinate. Intrinsic reaction coordinate (IRC) calculations were conducted to confirm that the transition states were found to connect the reactants and products. The relative stability of the different species was established by calculating their Gibbs free energy in solution at 298.15 K, which was used to describe the reaction profiles. Due to the well-known limitations of the harmonic oscillator model for low-frequency

vibrational modes thermal corrections were calculated by means of the Grimme approach for entropy [34] and the Head-Gordon method for enthalpy [35]. Atomic charges were calculated by fitting the molecular electrostatic potential with the Breneman and Wiberg [36] CHELPG scheme. Optimized coordinates of the structures together with energies are provided as Supplementary Material.

3.2. Experimental Details

3.2.1. Reagents

Dichloromethane was obtained from Sigma Aldrich and purified through an alumina column (Mbraun SPS). Trimethylene carbonate (TMC, 99.5%) was purchased from Actual Chemicals and purified by drying over calcium hydride, filtered under an inert atmosphere, and then recrystallised. The purified monomer was subsequently stored in a glove box. 4-Dimethylaminopyridine (DMAP, 99%) was purchased from Aldrich and co-evaporated three times with toluene followed by sublimation under vacuum at 85 °C and stored in a glovebox before use. Benzyl alcohol (99%, Aldrich) was dried over CaH₂, distilled under reduced pressure and stored in a glove box.

3.2.2. Polymerizations

TMC (1 g, 9.8 mmol), DMAP (12.0 mg, 0.098 mmol), benzyl alcohol (10.2 µL, 0.098 mmol) and 2 mL dichloromethane were added in a glass tube reactor and left to react at room temperature for 1 h. The reaction was then quenched with a solution of benzoic acid in dichloromethane. The resulting product was precipitated in methanol, filtered and dried for 48 h under vacuum.

3.2.3. Analytics

Size exclusion chromatography (SEC) was performed at a concentration of 2 g/L in THF as eluent at 40 °C using a Waters SIS HPLC-pump, a Waters 2414 refractometer, and Waters Styragel columns HR3 and HR4. The calibration was done using polystyrene standards (M_w 820, 2 727, 4 075, 12 860, 32 660, 45 730, 95 800, 184 200, 401 340 and 641 340 g/mol). ¹H NMR analyses were conducted in CDCl₃ at 25 °C with a Bruker AVANCE III HD 300 spectrometer at 300.13 MHz (7.05 Tesla). The conversion was determined by integration of the peak at 4.45 ppm and 4.23 ppm, corresponding to CH₂OCOO of the monomer and polymer respectively, and calculating $I_p/(I_m + I_p)$, where I_p and I_m are the values obtained for the integrals.

4. Conclusions

We have investigated in this study using computational methods the mechanisms of the ring-opening polymerization of TMC catalysed by DMAP and TBD and co-initiated by methanol. For both catalysts, a mechanism based on the activation of the alcohol co-initiator by the C=N moieties together with an H-bond between a proton of the catalyst and the carbonyl moieties of the monomer was found to lead to significantly lower energy barriers than the direct nucleophilic attack of the heterocyclic nitrogen molecule on the carbonate monomer, 11.3 and 25.7 vs. 23.7 and 90.3 kcal·mol^{−1} for TBD and DMAP, respectively. For both catalysts, we found the ring-opening of the TMC molecule as the rate-limiting step, slightly higher than the initial activated nucleophilic attack. The calculations also indicate TBD as a more efficient catalyst than DMAP, probably due to its polyfunctionality that allows simultaneous alcohol and carbonyl activation via conventional H-bonding on two different sites. The lower energy barriers found for TBD vs. DMAP were corroborated by ring-opening polymerization experiments conducted in dichloromethane at 25 °C.

Supplementary Materials: The following are available online at <https://www.mdpi.com/article/10.3390/catal12101280/s1>, Coordinates of selected structures presented in the Supplementary Materials section.

Author Contributions: Conceptualization, P.Z.; data curation, J.P.P.R.; formal analysis, M.L.-T., A.F.-H., J.P.P.R. and P.Z.; funding acquisition, W.T. and P.Z.; investigation, M.L.-T. and J.P.P.R.; methodology, J.P.P.R. and P.Z.; software, J.P.P.R.; supervision, A.F.-H., W.T. and P.Z.; writing—original draft, J.P.P.R. and P.Z.; writing—review & editing, A.F.-H., W.T., J.P.P.R. and P.Z. All authors have read and agreed to the published version of the manuscript.

Funding: This research was funded by Initiatives for Science, Innovation, Territories and Economy (I-SITE) Lille Nord—Europe and the APC was kindly offered by MDPI.

Data Availability Statement: Not applicable.

Acknowledgments: JPPR is grateful to the Fundação para a Ciência e a Tecnologia (FCT) for funding LAQV through projects UIDB/50006/2020 and UIDP/50006/2020. The authors are grateful to Aurélie Malfait for SEC measurements. The authors also acknowledge financial support from the Initiatives for Science, Innovation, Territories and Economy (I-SITE) Lille Nord—Europe (MLT PhD fellowship). Université de Lille, Chevreul Institute (FR 2638), Ministère de l'Enseignement Supérieur de la Recherche et de l'Innovation, Région Hauts-de-France are also acknowledged for supporting and funding partially this work.

Conflicts of Interest: The authors declare no conflict of interest.

References

- Artham, T.; Doble, M. Biodegradation of Aliphatic and Aromatic Polycarbonates: Biodegradation of Aliphatic and Aromatic Polycarbonates. *Macromol. Biosci.* **2008**, *8*, 14–24. [\[CrossRef\]](#) [\[PubMed\]](#)
- Xu, J.; Feng, E.; Song, J. Renaissance of Aliphatic Polycarbonates: New Techniques and Biomedical Applications: Review. *J. Appl. Polym. Sci.* **2014**, *131*, 39822. [\[CrossRef\]](#) [\[PubMed\]](#)
- Yu, W.; Maynard, E.; Chiaradia, V.; Arno, M.C.; Dove, A.P. Aliphatic Polycarbonates from Cyclic Carbonate Monomers and Their Application as Biomaterials. *Chem. Rev.* **2021**, *121*, 10865–10907. [\[CrossRef\]](#)
- Nederberg, F.; Lohmeijer, B.G.G.; Leibfarth, F.; Pratt, R.C.; Choi, J.; Dove, A.P.; Waymouth, R.M.; Hedrick, J.L. Organocatalytic Ring Opening Polymerization of Trimethylene Carbonate. *Biomacromolecules* **2007**, *8*, 153–160. [\[CrossRef\]](#) [\[PubMed\]](#)
- Helou, M.; Miserque, O.; Brusson, J.-M.; Carpentier, J.-F.; Guillaume, S.M. Organocatalysts for the Controlled “Immortal” Ring-Opening Polymerization of Six-Membered-Ring Cyclic Carbonates: A Metal-Free, Green Process. *Chem.—A Eur. J.* **2010**, *16*, 13805–13813. [\[CrossRef\]](#) [\[PubMed\]](#)
- Azemar, F.; Gimello, O.; Pinaud, J.; Robin, J.-J.; Monge, S. Insight into the Alcohol-Free Ring-Opening Polymerization of TMC Catalyzed by TBD. *Polymers* **2021**, *13*, 1589. [\[CrossRef\]](#) [\[PubMed\]](#)
- Lalanne-Tisné, M.; Eyley, S.; De Winter, J.; Favrelle-Huret, A.; Thielemans, W.; Zinck, P. Cellulose nanocrystals modification by grafting from ring opening polymerization of a cyclic carbonate. *Carbohydr. Polym.* **2022**, *295*, 119840. [\[CrossRef\]](#) [\[PubMed\]](#)
- Simón, L.; Goodman, J. The Mechanism of TBD-Catalyzed Ring-Opening Polymerization of Cyclic Esters. *J. Org. Chem.* **2007**, *72*, 9656–9662. [\[CrossRef\]](#)
- Bonduelle, C.; Martín-Vaca, B.; Cossío, F.P.; Bourissou, D. Monomer versus Alcohol Activation in the 4-Dimethylaminopyridine-Catalyzed Ring-Opening Polymerization of Lactide and LacticO-Carboxylic Anhydride. *Chem.—A Eur. J.* **2008**, *14*, 5304–5312. [\[CrossRef\]](#)
- Chuma, A.; Horn, H.W.; Swope, W.C.; Pratt, R.C.; Zhang, L.; Lohmeijer, B.G.G.; Wade, C.G.; Waymouth, R.M.; Hedrick, J.L.; Rice, J.E. The Reaction Mechanism for the Organocatalytic Ring-Opening Polymerization of L-Lactide Using a Guanidine-Based Catalyst: Hydrogen-Bonded or Covalently Bound? *J. Am. Chem. Soc.* **2008**, *130*, 6749–6754. [\[CrossRef\]](#)
- Katiyar, V.; Nanavati, H. Ring-opening polymerization of L-lactide using N-heterocyclic molecules: Mechanistic, kinetics and DFT studies. *Polym. Chem.* **2010**, *1*, 1491–1500. [\[CrossRef\]](#)
- Brown, H.A.; Waymouth, R.M. Zwitterionic Ring-Opening Polymerization for the Synthesis of High Molecular Weight Cyclic Polymers. *Accounts Chem. Res.* **2013**, *46*, 2585–2596. [\[CrossRef\]](#) [\[PubMed\]](#)
- Acharya, A.K.; Chang, Y.A.; Jones, G.O.; Rice, J.E.; Hedrick, J.L.; Horn, H.W.; Waymouth, R.M. Experimental and Computational Studies on the Mechanism of Zwitterionic Ring-Opening Polymerization of δ -Valerolactone with N-Heterocyclic Carbenes. *J. Phys. Chem. B* **2014**, *118*, 6553–6560. [\[CrossRef\]](#) [\[PubMed\]](#)
- Sherck, N.J.; Kim, H.C.; Won, Y.-Y. Elucidating a Unified Mechanistic Scheme for the DBU-Catalyzed Ring-Opening Polymerization of Lactide to Poly(Lactic Acid). *Macromolecules* **2016**, *49*, 4699–4713. [\[CrossRef\]](#)
- Nogueira, G.; Favrelle, A.; Bria, M.; Prates Ramalho, J.P.; Mendes, P.J.; Valente, A.; Zinck, P. Adenine as an Organocatalyst for the Ring-Opening Polymerization of Lactide: Scope, Mechanism and Access to Adenine-Functionalized Polylactide. *React. Chem. Eng.* **2016**, *1*, 508–520. [\[CrossRef\]](#)
- Stanley, N.; Chenal, T.; Jacquiel, N.; Saint-Loup, R.; Prates Ramalho, J.P.; Zinck, P. Organocatalysts for the Synthesis of Poly(Ethylene Terephthalate-Co-isosorbide Terephthalate): A Combined Experimental and DFT Study. *Macromol. Mater. Eng.* **2019**, *304*, 1900298. [\[CrossRef\]](#)

17. Nifant'ev, I.; Ivchenko, P. DFT Modeling of Organocatalytic Ring-Opening Polymerization of Cyclic Esters: A Crucial Role of Proton Exchange and Hydrogen Bonding. *Polymers* **2019**, *11*, 2078. [\[CrossRef\]](#)
18. Del Rosal, I.; Brignou, P.; Guillaume, S.M.; Carpentier, J.-F.; Maron, L. DFT Investigations on the Ring-Opening Polymerization of Cyclic Carbonates Catalyzed by Zinc- $\{\beta$ -Diiminate $\}$ Complexes. *Polym. Chem.* **2011**, *2*, 2564. [\[CrossRef\]](#)
19. Del Rosal, I.; Brignou, P.; Guillaume, S.M.; Carpentier, J.-F.; Maron, L. DFT Investigations on the Ring-Opening Polymerization of Substituted Cyclic Carbonates Catalyzed by Zinc- $\{\beta$ -Diketiminato $\}$ Complexes. *Polym. Chem.* **2015**, *6*, 3336–3352. [\[CrossRef\]](#)
20. Jitonnom, J.; Meelua, W. Effect of ligand structure in the trimethylene carbonate polymerization by cationic zirconocene catalysts: A “naked model” DFT study. *J. Organomet. Chem.* **2017**, *841*, 48–56. [\[CrossRef\]](#)
21. Kazarina, O.V.; Gourlaouen, C.; Karmazin, L.; Morozov, A.G.; Fedushkin, I.L.; Dagorne, S. Low valent Al(ii)–Al(ii) catalysts as highly active ϵ -caprolactone polymerization catalysts: Indication of metal cooperativity through DFT studies. *Dalton Trans.* **2018**, *47*, 13800–13808. [\[CrossRef\]](#) [\[PubMed\]](#)
22. Wei, J.; Riffel, M.N.; Diaconescu, P.L. Redox Control of Aluminum Ring-Opening Polymerization: A Combined Experimental and DFT Investigation. *Macromolecules* **2017**, *50*, 1847–1861. [\[CrossRef\]](#)
23. Xu, X.; Luo, G.; Mehmood, A.; Zhao, Y.; Zhou, G.; Hou, Z.; Luo, Y. Theoretical Mechanistic Studies on Redox-Switchable Polymerization of Trimethylene Carbonate Catalyzed by an Indium Complex Bearing a Ferrocene-Based Ligand. *Organometallics* **2018**, *37*, 4599–4607. [\[CrossRef\]](#)
24. Venkataraman, S.; Ng, V.W.L.; Coady, D.J.; Horn, H.W.; Jones, G.O.; Fung, T.S.; Sardon, H.; Waymouth, R.M.; Hedrick, J.L.; Yang, Y.Y. A Simple and Facile Approach to Aliphatic *N*-Substituted Functional Eight-Membered Cyclic Carbonates and Their Organocatalytic Polymerization. *J. Am. Chem. Soc.* **2015**, *137*, 13851–13860. [\[CrossRef\]](#)
25. Gregory, G.L.; Jenisch, L.M.; Charles, B.; Kociok-Köhn, G.; Buchard, A. Polymers from Sugars and CO₂: Synthesis and Polymerization of a D-Mannose-Based Cyclic Carbonate. *Macromolecules* **2016**, *49*, 7165–7169. [\[CrossRef\]](#)
26. Shen, Y.; Yang, X.; Song, Y.; Tran, D.K.; Wang, H.; Wilson, J.; Dong, M.; Vazquez, M.; Sun, G.; Wooley, K.L. Complexities of Regioselective Ring-Opening vs Transcarbonylation-Driven Structural Metamorphosis during Organocatalytic Polymerizations of Five-Membered Cyclic Carbonate Glucose Monomers. *JACS Au* **2022**, *2*, 515–521. [\[CrossRef\]](#)
27. Song, Y.; Yang, X.; Shen, Y.; Dong, M.; Lin, Y.-N.; Hall, M.B.; Wooley, K.L. Invoking Side-Chain Functionality for the Mediation of Regioselectivity during Ring-Opening Polymerization of Glucose Carbonates. *J. Am. Chem. Soc.* **2020**, *142*, 16974–16981. [\[CrossRef\]](#)
28. Li, S.; Lu, H.; Zhu, L.; Yan, M.; Kang, X.; Luo, Y. Ring-Opening Polymerization of L-Lactide Catalyzed by Food Sweetener Saccharin with Organic Base Mediated: A Computational Study. *Polymer* **2022**, *246*, 124747. [\[CrossRef\]](#)
29. Frisch, M.J.; Trucks, G.W.; Schlegel, H.B.; Scuseria, G.E.; Robb, M.A.; Cheeseman, J.R.; Scalmani, G.; Barone, V.; Petersson, G.A.; Nakatsuji, H.; et al. *Gaussian 16 Rev. B.01*; Gaussian, Inc.: Wallingford, CT, USA, 2016.
30. Zhao, Y.; Truhlar, D.G. The M06 suite of density functionals for main group thermochemistry, thermochemical kinetics, noncovalent interactions, excited states, and transition elements: Two new functionals and systematic testing of four M06-class functionals and 12 other functionals. *Theor. Chem. Acc.* **2008**, *120*, 215–241. [\[CrossRef\]](#)
31. Piletic, I.R.; Edney, E.O.; Bartolotti, L.J. Barrierless Reactions with Loose Transition States Govern the Yields and Lifetimes of Organic Nitrates Derived from Isoprene. *J. Phys. Chem. A* **2017**, *121*, 8306–8321. [\[CrossRef\]](#)
32. Peverati, R.; Truhlar, D.G. Quest for a Universal Density Functional: The Accuracy of Density Functionals across a Broad Spectrum of Databases in Chemistry and Physics. *Philos. Trans. R. Soc. A Math. Phys. Eng. Sci.* **2014**, *372*, 20120476. [\[CrossRef\]](#) [\[PubMed\]](#)
33. Marenich, A.V.; Cramer, C.J.; Truhlar, D.G. Universal Solvation Model Based on Solute Electron Density and on a Continuum Model of the Solvent Defined by the Bulk Dielectric Constant and Atomic Surface Tensions. *J. Phys. Chem. B* **2009**, *113*, 6378–6396. [\[CrossRef\]](#) [\[PubMed\]](#)
34. Grimme, S. Supramolecular Binding Thermodynamics by Dispersion-Corrected Density Functional Theory. *Chem. Eur. J.* **2012**, *18*, 9955–9964. [\[CrossRef\]](#) [\[PubMed\]](#)
35. Li, Y.-P.; Gomes, J.; Mallikarjun Sharada, S.; Bell, A.T.; Head-Gordon, M. Improved Force-Field Parameters for QM/MM Simulations of the Energies of Adsorption for Molecules in Zeolites and a Free Rotor Correction to the Rigid Rotor Harmonic Oscillator Model for Adsorption Enthalpies. *J. Phys. Chem. C* **2015**, *119*, 1840–1850. [\[CrossRef\]](#)
36. Breneman, C.M.; Wiberg, K.B. Determining Atom-Centered Monopoles from Molecular Electrostatic Potentials. The Need for High Sampling Density in Formamide Conformational Analysis. *J. Comput. Chem.* **1990**, *11*, 361–373. [\[CrossRef\]](#)